arXiv:1411.1556v2 [cond-mat.mtrl-sci] 30 Jun 2015

Facetted growth of Fe_3Si shells around GaAs nanowires on Si(111)

B. Jenichen,* M. Hilse, J. Herfort, and A. Trampert

Paul-Drude-Institut für Festkörperelektronik,

Hausvogteiplatz 5–7,D-10117 Berlin, Germany

(Dated: July 1, 2015)

Abstract

GaAs nanowires and GaAs/Fe_3Si core/shell nanowire structures were grown by molecular-beam epitaxy on oxidized Si(111) substrates and characterized by transmission electron microscopy. The surfaces of the original GaAs NWs are completely covered by magnetic Fe_3Si, exhibiting nanofacets and an enhanced surface roughness compared to the bare GaAs NWs. Shell growth at a substrate temperature of $T_S = 200$ °C leads to regular nanofacetted Fe_3Si shells. These facets, which lead to thickness inhomogeneities in the shells, consist mainly of well pronounced Fe_3Si(111) planes. The crystallographic orientation of core and shell coincide, i.e. they are pseudomorphic. The nanofacetted Fe_3Si shells found in the present work are probably the result of the Vollmer-Weber island growth mode of Fe_3Si on the {110} side facets of the GaAs NWs.

* bernd.jenichen@pdi-berlin.de

I. INTRODUCTION

Nanowires that combine a semiconductor and a ferromagnet in a core/shell geometry have gained a lot of interest in recent years.[1–6] Because of the cylindrical shape of the ferromagnet, such core/shell nanowires could allow for a magnetization along the wire and thus perpendicular to the substrate surface. Ferromagnetic stripes or tubes with a magnetization perpendicular to the substrate surface have the potential for circular-polarized light emitting diodes that can optically transmit spin information in zero external magnetic field.[7] This could enable three-dimensional magnetic recording with unsurpassed data storage capacities.[8, 9] The combination of the binary Heusler alloy Fe_3Si (Curie temperature of about 840 K) and GaAs, has several advantages compared to most previously studied semiconductor/ferromagnet (SC/FM) core/shell NWs. The perfect lattice matching allows for the molecular beam epitaxy (MBE) growth of high quality planar hybrid structures.[10–13] In addition, the cubic Fe_3Si phase shows a robust stability against stoichiometric variations, which only slightly modify the magnetic properties.[14] Moreover, the thermal stability against chemical reactions at the SC/FM interface is considerably higher than that of conventional ferromagnets like Fe, Co, Ni, and Fe_xCo_{1-x}. [10] We recently demonstrated that GaAs/Fe_3Si core/shell NWs prepared by MBE show ferromagnetic properties with a magnetization oriented along the NW axis (perpendicular to the substrate surface).[15] However, the structural and magnetic properties of the core/shell NWs were found to depend strongly on the substrate temperature during the growth of the Fe_3Si shells,[15, 16] and nanofacetting was observed.[16] In this work, we investigate periodically faceted Fe_3Si shells grown around GaAs(111) oriented cores and analyze the nanofacets by scanning electron microscopy (SEM), and transmission electron microscopy (TEM).

II. EXPERIMENT

GaAs/Fe_3Si core/shell NW structures were grown by MBE on Si(111) substrates. First, GaAs nanowires are fabricated by the Ga-assisted growth mode on Si(111) substrates covered with a thin native Si-oxide layer. The growth mechanism is the vapor-liquid-solid (VLS) mechanism,[17–21] where pin holes in the SiO_2 serve as nucleation sites.[22] A Ga droplet is the preferred site for deposition from the vapor. The GaAs NW then starts to grow by

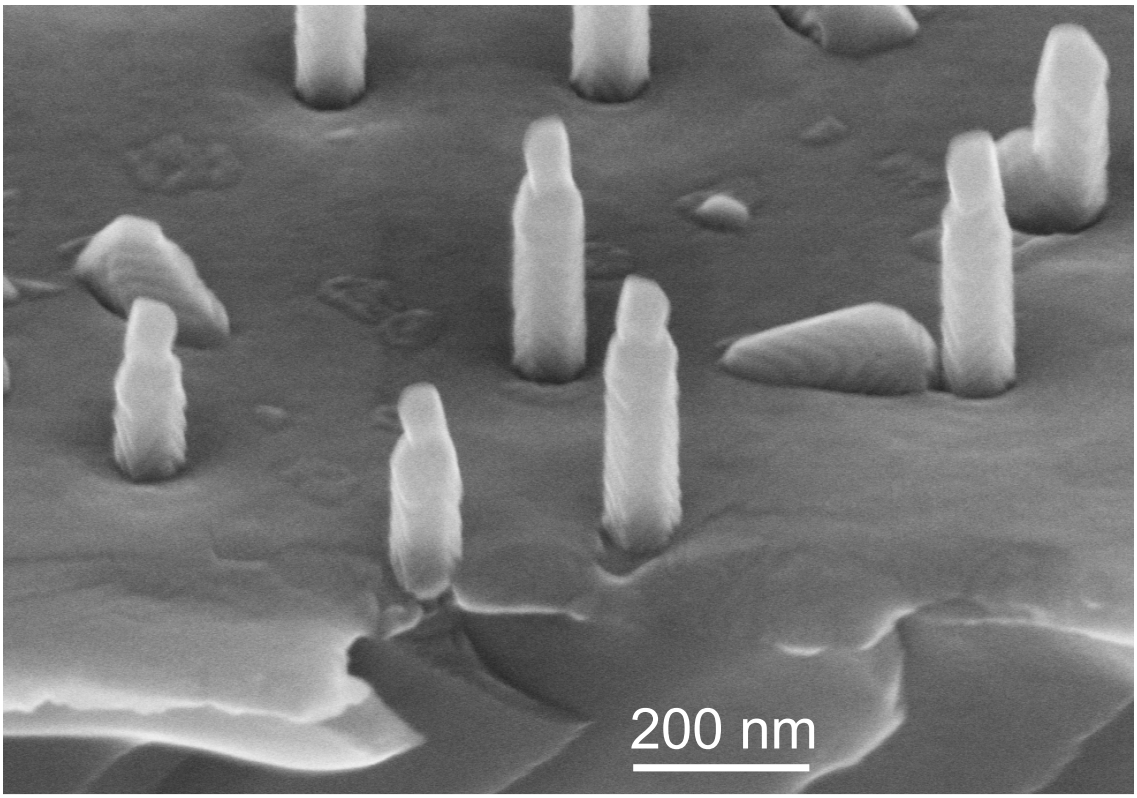

Figure 1. SEM image of GaAs/Fe_3Si core/shell NWs and islands grown by molecular beam epitaxy on a Si(111) substrate.

preferential nucleation at the spatially restricted GaAs/Si interface (IF). Further growth is nearly unidirectional and proceeds at the solid/liquid IF. The GaAs NWs are grown at a substrate temperature of 580 °C, with a V/III flux ratio of unity and an equivalent two-dimensional growth rate of 100 nm/h. Once the GaAs NW templates are grown, the sample is transferred under ultra high vacuum conditions to an As free growth chamber for deposition of the ferromagnetic films. There the GaAs NW templates were covered with Fe_3Si shells at substrate temperatures varying between 100 °C and 350 °C. The NW shells grown at 200 °C show a regular nanofacet structure and were selected for a careful analysis of the nanofacets. More details regarding the growth conditions can be found in Ref. [15].

The resulting core/shell NW structures were characterized by SEM and TEM. The TEM specimens are prepared by mechanical lapping and polishing, followed by argon ion milling according to standard techniques. TEM images are acquired with a JEOL 3010 microscope operating at 300 kV. The cross-section TEM methods provide high lateral and depth reso-

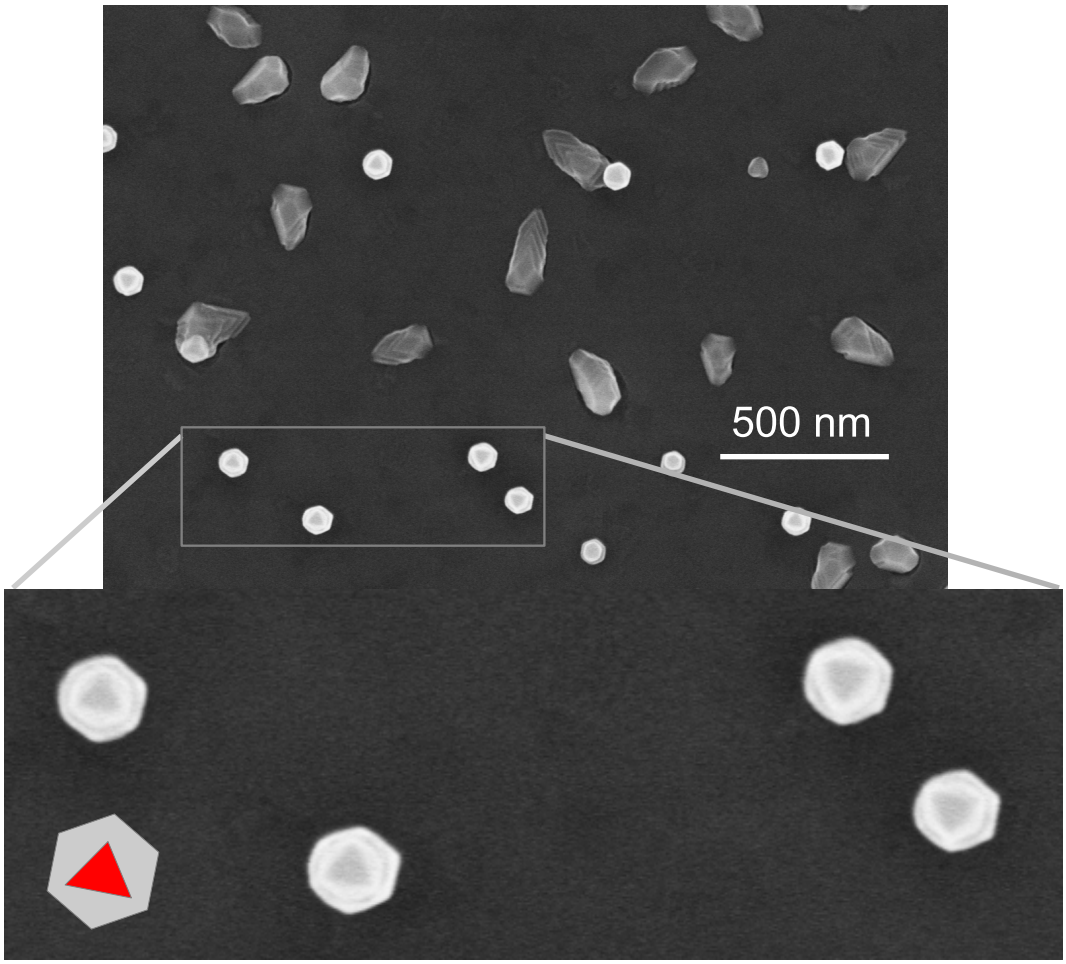

Figure 2. (color online) SEM top view of GaAs/Fe_3Si core/shell NWs and islands between the NWs grown by molecular beam epitaxy on a Si(111) substrate.

lutions on the nanometer scale, however they average over the thickness of the thin sample foil or the thickness of the NW as a whole.

III. RESULTS AND DISCUSSION

Figure 1 shows an SEM micrograph of the GaAs/Fe_3Si core/shell NWs. A relatively low area density of well oriented NWs of $\sim 5\times10^8$ cm^{-2} is found as well as a comparable density of hillhocks. During the last stage of GaAs NW growth no Ga is supplied, and so the remaining Ga in the droplet on top of the NWs is consumed, leading to an elongation of the NW at reduced diameter.[16] The sidewalls of the NWs exhibit nanofacetted surfaces. Figure 2 shows an SEM top view image of GaAs/Fe_3Si core/shell NWs grown by MBE

on a Si(111) substrate. The NWs exhibit the typical hexagonal cross-section (sketched in gray),[16] however, at higher magnification we observe triangular features (sketched in red) which are connected to the thinner necks of the NWs, where the tilted $Fe_3Si(111)$ planes form extended facets (cf. Fig. 1) intersecting the top $Fe_3Si(111)$ plane, which is parallel to the substrate surface. This results in the formation of the triangular features. The lower edges of the necks are more rounded.

Figure 3 shows a multi-beam bright-field TEM micrograph and corresponding SAD pattern, illustrating the orientational relationship of a GaAs/Fe_3Si core/shell NW on Si(111). We observe a coincidence of the core- and shell-orientations, hence the Fe_3Si growth is predominantly epitaxial on the GaAs. In addition, the crystallographic orientation of the Fe_3Si shell was confirmed by high-resolution TEM (not shown here). The grey line drawn on the SAD pattern near the $11\bar{1}$ reflection is oriented perpendicular to the Fe_3Si nanofacets visible in the corresponding micrograph. The separation of the diffraction spots along this line corresponds to the (111) net plane distance of Fe_3Si and indicates the nanofacets are mainly (111)-oriented. In the SAD pattern from a single core/shell NW the Fe_3Si maxima are stronger probably due to the larger volume fraction of the shell. In order to measure the SAD, the substrate was first oriented near the [011] zone axis. Then the sample had to be tilted a little further in order to reach the [011] zone axis of the GaAs NW, since the axis of the NW was not exactly perpendicular to the Si surface. In the NW SAD pattern shown in Fig. 3 the fundamental reflections of the Fe_3Si are more intense than the super-lattice maxima.[11] Nevertheless we can distinguish, $2\bar{2}2$, $3\bar{3}3$, and $4\bar{4}4$ maxima indicating the NW is properly oriented and the crystallographic orientations of core and shell basically coincide. This illustrates that a growth temperature of 200 °C results in a highly perfect Fe_3Si shell structure. The surface nanofacets are inclined to the (111) net planes parallel to the Si surface by an angle of approximately 108°. The formation of facets reduces the overall surface energy and evidences non negligible material transport over distances small compared to the NW lengths.[23, 24] Unfortunately, the orientation of those surface nanofacets does not coincide with the GaAs NWs facets corresponding to {110} planes.[25] As a result, the facetted growth leads to shell thickness inhomogeneity. On a larger length-scale the Fe_3Si shell is approximately reproducing the shape of the GaAs core NWs.[16]

Layer-by-layer growth could in principle solve the problem of nanofacetting. However, even planar Fe_3Si grows on GaAs(001) in the Vollmer-Weber (VW) island growth mode.[26]

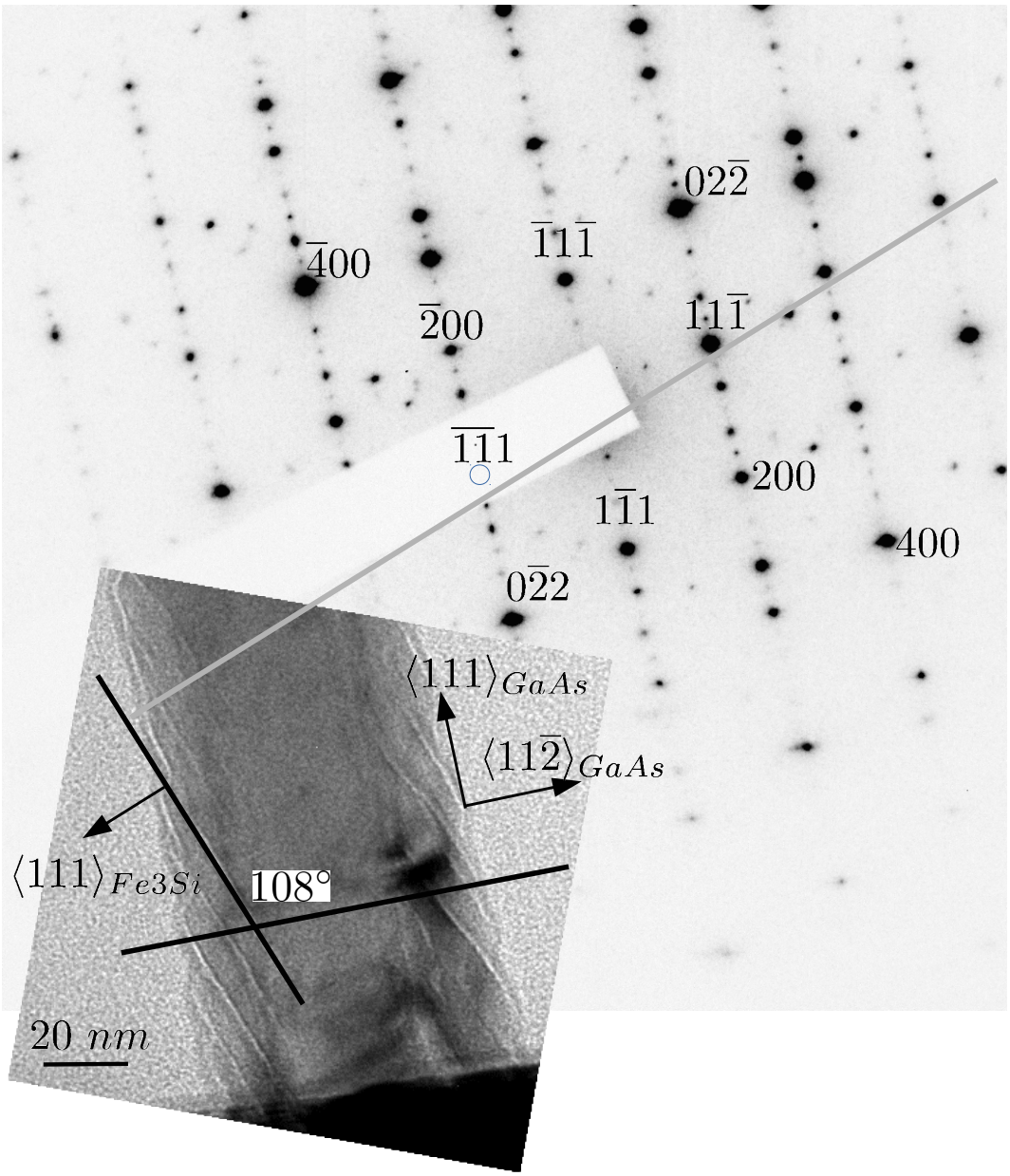

Figure 3. Multi-beam bright-field TEM micrograph and the corresponding SAD pattern illustrating the orientational relationship of a GaAs/Fe_3Si core/shell NW. The straight line near the $11\bar{1}$ reflection is oriented perpendicular to the nanofacets of Fe_3Si visible in the corresponding micrograph.

Poor wetting during the growth of Fe_3Si on GaAs leads initially to isolated islands, despite of perfect lattices match. We speculate that the nanofacetted Fe_3Si shells found in the present work are a result of VW island growth. One way to improve the homogeneity and other structural properties of Fe_3Si-shells could be to use surfactants. For planar growth on GaAs,

surfactant materials like Sb [27], Bi [28] and Te [29] have been investigated.

IV. CONCLUSIONS

GaAs core NWs were grown epitaxially on the oxidized Si(111) surface (inside holes of the SiO_2 film) via the VLS growth mechanism. Then magnetic Fe_3Si shells were grown resulting in continuous covering of the cores. Fe_3Si shells grown at a substrate temperature of $T_S =$ 200 °C are fully epitaxial with a nanofacetted surface. The $(\bar{1}11)$ facets are most pronounced, forming a regular pattern around the GaAs NWs. This facetting is probably the result of the VW island growth mode of Fe_3Si on GaAs.

V. ACKNOWLEDGEMENT

The authors thank Claudia Herrmann for her support during the MBE growth, Doreen Steffen for sample preparation, Astrid Pfeiffer for help in the laboratory, Anne-Kathrin Bluhm for the SEM micrographs, Ryan Lewis, Esperanza Luna and Uwe Jahn for valuable support and helpful discussion.

VI. REFERENCES

[1] M. Hilse, Y. Takagaki, J. Herfort, M. Ramsteiner, C. Herrmann, S. Breuer, L. Geelhaar, and H. Riechert, Appl. Phys. Lett. **95**, 133126 (2009).

[2] A. Rudolph, M. Soda, M. Kiessling, T. Wojtowicz, D. Schuh, W. Wegscheider, J. Zweck, C. Back, and E. Reiger, Nano Lett. **9**, 3860 (2009).

[3] D. Rueffer, R. Huber, and P. Berberich, Nanoscale **4**, 4989 (2012).

[4] N. S. Dellas, J. Liang, B. J. Cooley, N. Samarth, and S. E. Mohney, Appl. Phys. Lett. **97**, 072505 (2010).

[5] K. Tivakornsasithorn, R. E. Pimpinella, V. Nguyen, X. Liu, M. Dobrowolska, and J. K. J. Furdyna, J. Vac. Sci. Technol. B **30**, 02115 (2012).

[6] X. Yu, H. Wang, D. Pan, J. Zhao, J. Misuraca, S. Molnar, and P. Xiong, Nano Lett. **13**, 1572 (2013).

[7] R. Farshchi, M. Ramsteiner, J. Herfort, A. Tahraoui, and H. T. Grahn, Appl. Phys. Lett. **98**, 162508 (2011).

[8] S. S. Parkin, M. Hayashi, and L. Thomas, Science **320**, 190 (2008).

[9] K. S. Ryu, L. Thomas, S. H. Yang, and S. S. Parkin, Appl. Phys. Exp. **5**, 093006 (2012).

[10] J. Herfort, H.-P. Schönherr, and K. H. Ploog, Appl. Phys. Lett. **83**, 3912 (2003).

[11] B. Jenichen, V. M. Kaganer, J. Herfort, D. K. Satapathy, H. P. Schönherr, W. Braun, and K. H. Ploog, Phys. Rev. B **72**, 075329 (2005).

[12] J. Herfort, B. Jenichen, V. Kaganer, A. Trampert, H. P. Schoenherr, and K. Ploog, Physica E **32**, 371 (2006).

[13] J. Herfort, A. Trampert, and K. Ploog, Int. J. Mater. Res. **97**, 1026 (2006).

[14] J. Herfort, H. P. Schoenherr, K. J. Friedland, and K. H. Ploog, J. Vac. Sci. Technol. B **22**, 2073 (2004).

[15] M. Hilse, J. Herfort, B. Jenichen, A. Trampert, M. Hanke, P. Schaaf, L. Geelhaar, and H. Riechert, Nano Lett. **13**, 6203 (2013).

[16] B. Jenichen, M. Hilse, J. Herfort, and A. Trampert, J. Cryst. Growth, in press **409**.

[17] R. S. Wagner and W. S. Ellis, Appl. Phys. Lett. **4**, 89 (1964).

[18] B. Mandl, J. Stangl, T. Martensson, A. Mikkelsen, J. Eriksson, L. S. Karlsson, G. Bauer, L. Samuelson, and W. Seifert., Nano Lett. **6**, 1817 (2006).

[19] F. Glas, J. C. Harmand, and G. Patriarche, Phys. Rev. Lett. **99**, 146101 (2007).

[20] A. Fontcuberta, C. Colombo, G. Abstreiter, J. Arbiol, and J. R. Morante, Appl. Phys. Lett. **92**, 063112 (2008).

[21] B. A. Wacaser, K. A. Dick, J. Johansson, M. T. Borgstroem, K. Deppert, and L. Samuelson, Advanced Materials **21**, 153 (2009).

[22] S. Breuer, C. Pfueller, T. Flissikowski, O. Brandt, H. T. Grahn, L. Geelhaar, and H. Riechert, Nano Lett. **11**, 1276 (2011).

[23] G. V. Wulff, Z. Kristallogr. **34**, 449 (1901).

[24] eds: G. Dhanaraj, K. Byrappa, V. Prasad, and M. Dudley, "Handbook of crystal growth," (Springer, Berlin, Heidelberg, 2010) p. 58.

[25] J. Grandal, M. Wu, X. Kong, M. Hanke, E. Dimakis, L. Geelhaar, H. Riechert, and A. Trampert, Appl. Phys. Lett. **105**, 121602 (2014).

[26] V. M. Kaganer, B. Jenichen, R. Shayduk, W. Braun, and H. Riechert, Phys. Rev. Lett. **102**, 016103 (2009).

[27] T. Kageyama, T. Miyamoto, M. Ohta, T. Matsuura, Y. Matsui, T. Furuhata, and F. Koyama, J. Appl. Phys. **96**, 44 (2004).

[28] S. Tixier, M. Adamcyk, E. Youngb, J. Schmid, and T. Tiedje, J. Cryst. Gr. **251**, 449 (2003).

[29] N. Grandjean, J. Massies, and V. H. Etgens, Phys. Rev. Lett. **69**, 796 (1992).